Journal of Crystal Growth xxx (2017) xxx-xxx

Contents lists available at ScienceDirect

Journal of Crystal Growth

journal homepage: www.elsevier.com

Growth study of self-assembled GaN nanocolumns on silica glass by plasma assisted molecular beam epitaxy

Andreas Liudi Mulyo[a, b, *], Yuta Konno[b], Julie S. Nilsen[c], Antonius T.J. van Helvoort[c], Bjørn-Ove Fimland[a], Helge Weman[a, b], Katsumi Kishino[b, d]

[a] Department of Electronic Systems, Norwegian University of Science and Technology (NTNU), NO-7491 Trondheim, Norway
[b] Department of Engineering and Applied Sciences, Sophia University, 7-1 Kioi-cho, Chiyoda-ku, Tokyo 102-8554, Japan
[c] Department of Physics, Norwegian University of Science and Technology (NTNU), NO-7491 Trondheim, Norway
[d] Sophia Nanotechnology Research Center, Sophia University, 7-1 Kioi-cho, Chiyoda-ku, Tokyo 102-8554, Japan

ARTICLE INFO

Keywords:
A1. Nanostructures
A3. Molecular beam epitaxy
B1. Nitrides
B1. Glasses
B2. Semiconducting III–V materials

ABSTRACT

We demonstrate GaN nanocolumn growth on fused silica glass by plasma-assisted molecular beam epitaxy. The effect of the substrate temperature, Ga flux and N_2 flow rate on the structural and optical properties are studied. At optimum growth conditions, GaN nanocolumns are vertically aligned and well separated with an average diameter, height and density of 72 nm, 1.2 μm and $1.6\times10^9\,cm^{-2}$, respectively. The nanocolumns exhibit wurtzite crystal structure with no threading dislocations, stacking faults or twinning and grow in the [0 0 0 1] direction. At the interface adjacent to the glass, there is a few atom layers thick intermediate phase with *ABC* stacking order (zinc blende). Photoluminescence measurements evidence intense and narrow excitonic emissions, along with the absence of any defect-related zinc blende and yellow luminescence emission.

1. Introduction

Wide band-gap GaN and related ternary III-N semiconductor compounds have been recognized to be among the most important semiconductors for electronic [1,2] and optoelectronic devices [3–5] due to their remarkable optical, electrical and physical properties [1,5]. Nevertheless, the commercialization of GaN-based devices is hampered by the limitation of substrate availability. Si and sapphire (Al_2O_3) have been traditionally employed for the reason of low-cost and good thermal conductivity, despite of having a relatively large lattice- and thermal expansion-mismatch with GaN [6]. This results in a high stacking fault density that affects the efficiency negatively. An alternative could be SiC which offers smaller lattice mismatch for *c*-GaN epitaxy as well as a higher thermal conductivity [6]. However, its poor wetting with GaN, rough surface and high cost [6] inhibit SiC to be fully exploited for GaN-based devices.

The bottom-up growth of nanocolumns (NCs) offers new opportunities to obtain high quality heteroepitaxial material [7–11]. Lattice mismatch is accommodated via the small NC footprint on the substrate, which induces elastic, rather than plastic, strain relaxation at the free surface extending into the NC volume. The generated strain and possible misfit dislocations are confined to the NC/substrate interface and not affecting the bulk of the NC. [12]. Thus, the crystal quality of the epitaxial material is nearly independent of the crystalline characteristics of the underlying substrate [13,14]. As a consequence of its large aspect ratio [15–18], possible dislocation lines for NC whose diameter exceeds its critical diameter [7] tend to find its minimum energy by shortening its length in such a way that it bends towards the NC sidewalls instead of propagating vertically along [0 0 0 1] [18]. This explains why the strain relaxation is observed at the lower sidewall facets of NCs [7,19], allowing the upper part of the NC to be free from structural defects [15–18,20]. This merit is exploited in GaN NC growth on various types of substrate material, from crystalline (Si [8,21] and Al_2O_3 [8,22,23]), amorphous (SiO_2 [24–26], SiN [27], Al_xO_y [28] and TiN [29]) and metal foil (Ti [30,31]). Moreover, high quality GaN NCs have been successfully grown both on multi-layer graphene on SiO_2/Si(1 0 0) substrate covered with a thin AlN buffer layer by molecular beam epitaxy (MBE) [32] and directly on single-layer graphene using metal-organic vapor phase epitaxy (MOVPE) [33].

Fused silica glass is an attractive substrate, not only because it is cheap but it also has an excellent optical transparency in the visible and ultraviolet wavelength region [34]. GaN growth on fused silica was demonstrated by Iwata et al. already in 1997 [35], but the GaN layers were highly polycrystalline in nature [36]. Despite this, the optical properties showed a favorable indication for the fabrication of large area and low-cost light emitting diodes (LEDs) and solar cells [35–38]. Subsequently, there have been several works investigating morphologies and photoluminescence properties of GaN grown on non-single

* Corresponding author at: Department of Electronic Systems, Norwegian University of Science and Technology (NTNU), NO-7491 Trondheim, Norway.
Email address: andreas.liudi-mulyo@ntnu.no (A.L. Mulyo)

https://doi.org/10.1016/j.jcrysgro.2017.10.009
Received 26 May 2017; Received in revised form 17 September 2017; Accepted 7 October 2017
Available online xxx
0022-0248/

crystalline or amorphous substrates by either MBE or MOVPE [39–41]. Moreover, fabrication of GaN-based optoelectronic devices [42] exploiting such substrates have been realized with promising performances. Recently, high density and vertically aligned single crystal GaN NCs on fused silica have been demonstrated [13]. To further optimize and utilize this result, it is important to have a detailed understanding on the effect of various growth conditions, in order to optimize the crystalline quality of the GaN NCs and achieve high internal quantum efficiency, which are essential to enhance device efficiency.

This paper presents a growth study of self-assembled GaN NCs on fused silica by plasma-assisted molecular beam epitaxy (PA-MBE). Substrate temperature (T_{sub}), Ga flux (Φ_{Ga}) and N_2 flow rate (Q_N) are varied in order to study their influence upon the structural and optical characteristics of the GaN NCs. The grown GaN NCs are studied using scanning electron microscopy (SEM) and room-temperature (RT) micro-photoluminescence (μ-PL) spectroscopy. Furthermore, the optimized growth of GaN NCs is investigated with lattice-imaging (scanning) transmission electron microscopy (HRTEM and HRSTEM) and μ-PL spectroscopy at 77 K (77 K μ-PL).

2. Experiments

The GaN NCs were grown on 2" fused silica wafers from Semiwafer (thickness of 0.5 mm with a purity of 99.999%) using PA-MBE under N-rich conditions. Standard Knudsen effusion cells were used to supply Ga and Si atoms, while atomic nitrogen was generated from a radio-frequency plasma source operating at 450 W. A 300 nm thick Ti film was evaporated on the backside of the fused silica wafer to ensure a uniform and efficient heat transfer from the heater to the substrate as well as assist pyrometer reading. Prior to loading to the growth chamber, the substrate was thermally cleaned at 350 °C for 1 h in a preparation chamber. Catalyst-free, self-assembled GaN NCs were then grown directly on fused silica, without deliberately forming any intermediate buffer layer. The growth process was initiated by opening the Ga and N_2 shutters simultaneously, i.e. no intentional nitridation took place on the surface of the substrate prior to NC growth. The GaN NCs were n-type doped with Si using a cell temperature of 1050 °C and a growth time of 90 min, identical for all growth series. Si doping has been reported to improve the optical properties of GaN layers [43] based on the capability of Si to decrease dislocation density [44]. Its solubility in GaN films is high, of the order of $10^{20}\,cm^{-3}$, and free carrier concentrations in the range from 10^{17} to $2\times10^{19}\,cm^{-3}$ have been reported [45]. Table 1 lists the growth conditions of each sample grown for this study.

The structure of the as-grown samples (i.e. without a thin metal coating to reduce charging effects from a high resistivity of the fused silica substrate) was evaluated using a SMI3050SE SEM operating at 15 kV. The optical properties were assessed with RT and 77 K μ-PL using a HeCd laser (325 nm) as excitation source. A commercial GaN bulk substrate grown by hydride vapor phase epitaxy is set as a benchmark reference (HVPE-GaN) of the optical quality, like for previous studies on NC growth on different substrates [15,32]. To verify the crystalline quality of the optimized GaN NCs, different TEM imaging methods (selective area diffraction (SAED), HRTEM, high-angle annular dark field scanning TEM (HAADF STEM)) using a field emission JEOL-2100F and JEOL JEM-ARM200F, both operating at 200 kV, have been used. The TEM specimen was made by a lift-out method utilizing a focused ion beam (FIB). Prior to FIB, the NCs were coated with Au in order to avoid electron charging during the FIB specimen preparation. The TEM lamella was not coated for the TEM analysis.

3. Results and discussion

A summary of the grown GaN NC diameter and density for samples FS001 to FS008 is shown in Fig. 1. The alteration in NC morphology, diameter and density for each sample corresponds to the given growth conditions as described in Table 1.

SEM images of the GaN NCs grown at different T_{sub} are presented in Fig. 2. At 730 °C (sample FS001), the GaN growth resembles a thin film, although it does not cover the whole surface. When T_{sub} is increased to 750 °C (sample FS002), the coalescence is reduced, giving a good indication of further NC isolation. For the sample grown at 760 °C (sample FS003), the formation of NCs becomes clearly visible. Accordingly, the NC density in sample FS003 is increased as its average diameter is decreased relative to sample FS002 (Fig. 1). Higher T_{sub} increases significantly the likelihood of Ga desorption and GaN decomposition [46]. At the same time, Ga diffusion length is enhanced, which becomes a driving factor for the Ga atoms to have a higher probability in reaching the top of the NC *c*-plane [47]. The V/III ratio should thus play an important role for the columnar morphology [46].

The dependence of the GaN columnar morphology on Φ_{Ga}, is shown in Fig. 3. We expect that growth at a reduced Ga supply, especially at a very high T_{sub}, leads to a limited amount of Ga availability on the surface, restricting GaN formation and eventually suppressing the degree of NC coalescence. The growth using Φ_{Ga} of 3.0×10^{-4} Pa is seen to result in coalescence between NCs (sample FS003), whereas the columnar structure becomes more apparent when Φ_{Ga} is reduced to a lower flux. The average diameter has decreased to 72 nm while the density is lowered to $1.6\times10^{9}\,cm^{-2}$ (Fig. 1) at Φ_{Ga} of 2.5×10^{-4} Pa sample FS006). However, larger and more diverse NC diameters (80–160 nm, see Fig. 1) are observed when Φ_{Ga} is lowered to 2.0×10^{-4} Pa (sample FS004). Further investigation is needed to verify this phenomenon and provide a plausible explanation regarding the inconsistency found for a low Φ_{Ga}.

To investigate the effect of N atoms in contributing to the NCs growth, Q_N is varied and the SEM results are presented in Fig. 4. In general, a columnar structure can be obtained using Q_N ranging from 1.50 to 2.75 sccm. The electron charging effect due to the high electrical resistivity of fused silica becomes evident in SEM on the sample grown with the lowest Q_N (sample FS008) when it is observed in bird view. This is due to that this sample has a relatively low density of NCs and that the SEM detector in this imaging angle receives information mostly from the charging substrate surface.

It is noticeable from Fig. 4(a–f) that both the NC density and diameter are reduced with a lower Q_N, implying that Ga desorption is enhanced. There is also a significant variation of the NC height, where the highest NCs are found on FS006 (1220 ± 35 nm), followed by FS007 (870 ± 70 nm) and FS008 (540 ± 100 nm). The radial and axial growth rates are reduced with a lower Q_N, resulting in shorter and thinner NCs. In addition, the distance between NCs become larger, hence the number density is decreased (Fig. 4(c–d), (e–f) and Fig. 1). Compared to FS006, a larger variation in length and diameter (Fig. 1) is observed for FS007 and FS008 (NCs grown at lower Q_N, Fig. 4(d), (f)). This indicates that individual GaN NCs experience different nucleation times, similar to what is reported by Wölz et al. [29] for GaN NC growth on metallic TiN films. When Q_N is 2.75 sccm, a finer NC structure is obtained, confirmed by the uniformity of the NC diameter, density and height (Fig. 4(a), (b)), implying that the NCs nucleate at an early stage, almost simultaneously. A comprehensive nucleation study is beyond the scope of this work and will be reported elsewhere. A cross-sectional HAADF STEM image of FS006 shows that the en-

Table 1
GaN nanocolumn growth conditions for the different samples used in this study.

Sample ID	FS001	FS002	FS003	FS004	FS006	FS007	FS008
T_{sub} (°C)	730	750	760	760	760	760	760
Φ_{Ga} (Pa)	3.0×10^{-4}	3.0×10^{-4}	3.0×10^{-4}	2.0×10^{-4}	2.5×10^{-4}	2.5×10^{-4}	2.5×10^{-4}
Q_N (sccm)	2.75	2.75	2.75	2.75	2.75	2.00	1.50

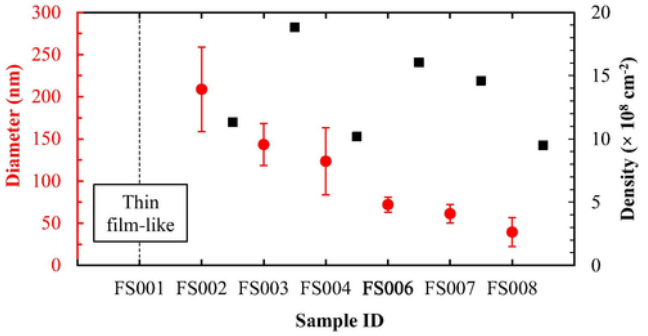

Fig. 1. Diameter (red dots) and density (black squares) of the grown GaN NCs on samples FS001 to FS004 and FS006 to FS008. (For interpretation of the references to colour in this figure legend, the reader is referred to the web version of this article.)

semble of NCs grow near perpendicular to the fused silica substrate, where each NC has a flat top facet and smooth sidewalls (Fig. 4(g)).

An overview of the optical quality of all samples is given in Fig. 5. Overall, the RT μ-PL measured in the range from 340 to 580 nm displays a single emission peak at 364 nm in all samples, due to the wurtzite GaN free exciton emission.

As shown in Fig. 5, the PL peak intensity of the first four samples (FS001–FS004) are below that of the HVPE-GaN reference sample. However, the PL intensity increases gradually with higher sample ID number, which can be reasoned from that higher T_{sub} (for FS001–FS003, see Table 1) aids in effectively decreasing the stacking fault density [48] (coalesced NCs are minimized [20]). A higher light extraction efficiency (LEE) is demonstrated through non-coalescence NC structure by sample FS004 upon reducing Φ_{Ga}. In addition, it has a full width at half maximum (FWHM) of 67.4 meV, which is much narrower than for samples FS001 to FS003 (Fig. 5). A significant improvement is found in sample FS006, where the PL peak intensity is at least three times higher than for the HVPE-GaN reference sample, demonstrating a similar quality as reported for self-organized GaN NCs on graphene [32]. In addition, it has the lowest FWHM (67 meV) of all samples in this study (Fig. 5). The PL intensity

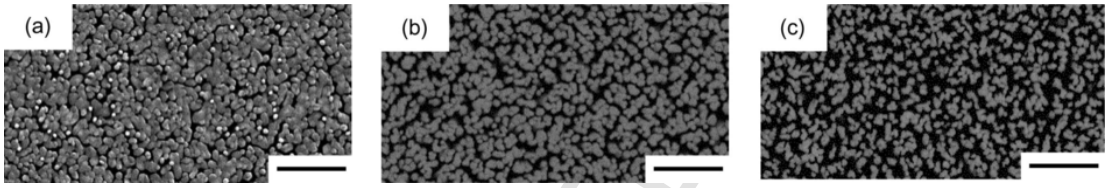

Fig. 2. Top view SEM images of GaN NC growth at different T_{sub} ((a) 730 °C (FS001), (b) 750 °C (FS002) and (c) 760 °C (FS003)). Φ_{Ga} and Q_N are fixed to 3.0×10^{-4} Pa and 2.75 sccm, respectively. All scale bars are 1 μm.

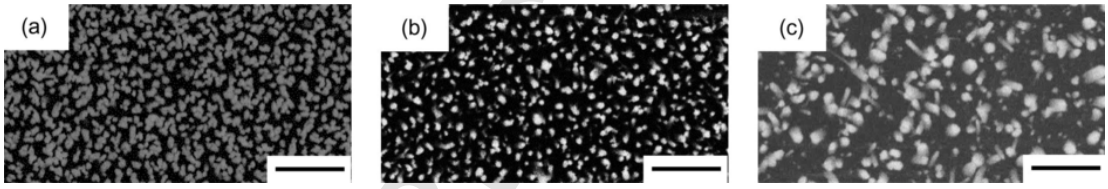

Fig. 3. Top view SEM images of GaN NC growth at different Φ_{Ga} ((a) 3.0×10^{-4} Pa (FS003), (b) 2.5×10^{-4} Pa (FS006) and (c) 2.0×10^{-4} Pa (FS004)). T_{sub} and Q_N, are fixed to 760 °C and 2.75 sccm, respectively. All scale bars are 1 μm.

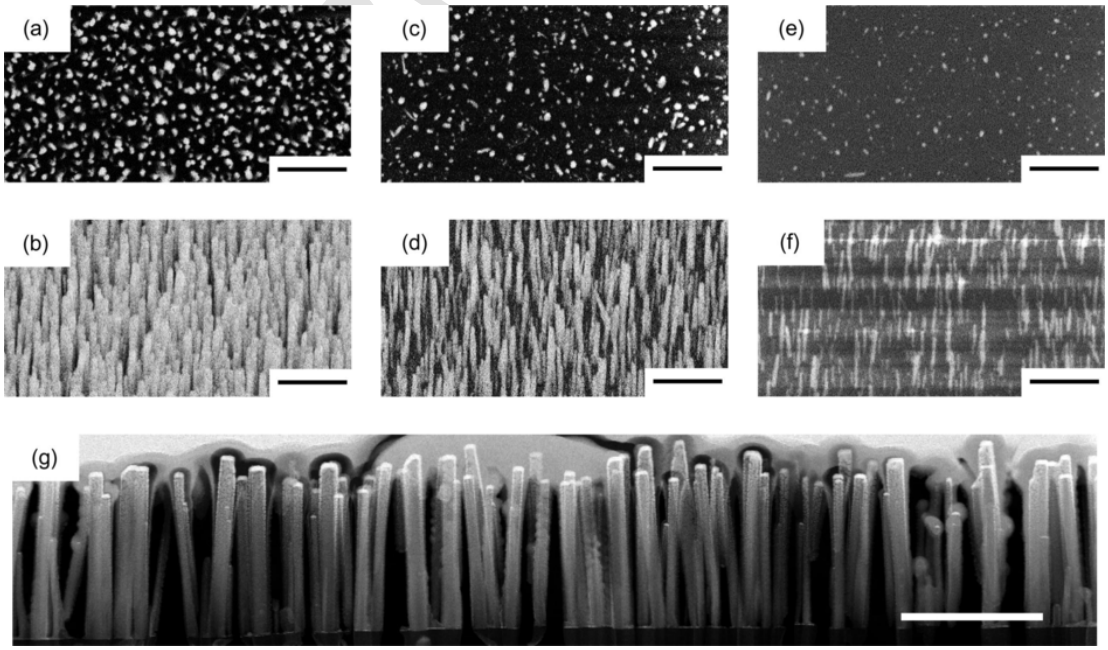

Fig. 4. SEM images (top and bird view at top and middle row, respectively) of GaN NC growth with different Q_N ((a, b) 2.75 sccm (FS006), (c, d) 2.00 sccm (FS007) and (e, f) 1.50 sccm (FS008)). T_{sub} and Φ_{Ga} are fixed to 760 °C and 2.5×10^{-4} Pa, respectively. (g) A HAADF STEM overview image of FS006 (a, b). All scale bars are 1 μm.

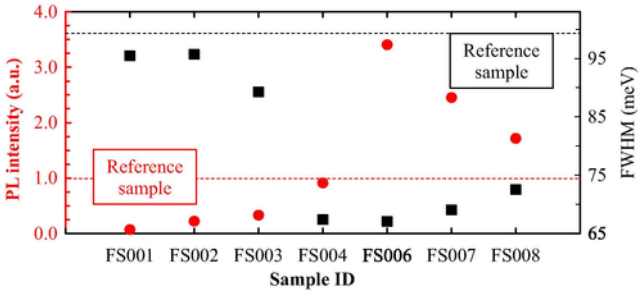

Fig. 5. RT μ-PL maximum peak intensity (red dots) and FWHM (black squares) of grown GaN NCs. The PL peak emission at 364 nm has been normalized to the peak intensity from the HVPE-GaN reference sample. The PL intensity and FWHM of the HVPE-GaN reference sample are indicated by the dashed red and black lines, respectively. (For interpretation of the references to colour in this figure legend, the reader is referred to the web version of this article.)

is further reduced when the Q_N is decreased to 2.00 and 1.50 sccm in sample FS007 and FS008, respectively. The grown NCs in sample FS007 and FS008 are observed to have a larger diameter and height dispersion, as well as lower density compared with FS006 (Figs. 1 and 4(a–f)). We expect that these factors are the main reasons for the lower LEE in FS007 and FS008 [15]. From structural and optical evaluations, it can thus be deduced that sample FS006 has the highest quality among all grown NCs on fused silica, and its quality is on par with the GaN NCs on different substrates [15,32]. Further detailed examinations by TEM, RT and 77 K μ-PL on this sample are presented below.

The crystallinity of NC and its interface with the fused silica substrate is unveiled by HRTEM, as shown in Fig. 6(a). The SAED image (inset in Fig. 6(a)) shows that the NC has a wurtzite crystal structure and the growth direction is [0 0 0 1]. Even though fused silica is a non-crystalline material, the grown NC is vertical and consistently demonstrates a single crystalline structure with well-defined atomic planes. A darker irregular layer is clearly seen at the interface. This suggests the formation of a thin interfacial layer with a thickness of about 0–4 atomic layers. By aberration corrected HAADF STEM (lower inset in Fig. 6(b)), the atom columns in the interfacial layer seems less bright compared to the rest of the NC. Assuming an equal specimen thickness, which is reasonable for a FIB specimen, this indicates that this layer has a lower average atomic number, which could indicate that it is Si_xN_y rather than GaN. Due to charging effects, energy-dispersive X-ray spectroscopy could not be performed to confirm the composition of this layer.

In addition, the fact that Si-N (4.5 eV) has a higher bonding energy compared to Ga-N (2.2 eV), favors SiN rather than GaN as the origin of the interface layer [24]. The layer has a zinc blende crystal structure (*ABC* stacking order, lower inset in Fig. 6(b)) observed in this interface region. The crystalline interfacial layer with an *ABC* stacking might therefore be Si_xN_y. Due the small and varying layer thickness, i.e. between 0–4 atomic layers, analyzing this layer becomes more challenging. Albeit being inconclusive regarding the exact composition, the variation in stacking order is a clear indication of another phase at the interface. To further study this interfacial layer would require a solution for the charging problem to allow a dedicated advanced TEM study. The stacking otherwise reveals an *ABAB* order (upper inset in Fig. 6(b)), an evidence of wurtzite crystal structure excluding structural defects, such as threading dislocations and stacking faults. These results serve as a clear evidence of the high structural quality of the GaN NC under investigation (sample FS006), despite it is grown on an amorphous substrate. These results demonstrate the superiority of GaN NC crystal quality over a thin film structure [35,49].

This interfacial layer is generally observed in the grown GaN NCs on Si, both intentionally [27,50,51] and unintentionally grown [14,47,52–54]. However, these reported studies (except [53] which used reflection high energy-electron diffraction and *in situ* grazing incidence X-ray diffraction) on cross-sectional lattice imaging were done solely by HRTEM, making stacking order interpretation of a thin (i.e. a few atomic layers thick) interfacial layer difficult [55], and they did not further discuss the stacking order.

RT μ-PL measurements in the range from 340 to 580 nm of a HVPE-GaN reference sample (black line) and an ensemble GaN NCs (sample FS006, red line) are presented in Fig. 7(a). Both samples exhibit band edge emission from the GaN wurtzite crystal phase at 364 nm, with a small additional shoulder (grey arrow) observed in the HVPE-GaN reference sample. The NC structure (red line) has an intensity of 3.3 times higher compared to the thin film reference (black line). Zinc blende GaN-related emission, typically occurring at 386 nm [56], is not observed. In addition, the HVPE-GaN reference sample clearly shows PL corresponding to broad yellow luminescence (YL) emission (see insets of Fig. 7(a)). This infamous broad luminescence in GaN could be caused by the deep acceptor level introduced by the Ga vacancy [57–59] or C substituting Ga (C_{Ga}) [57,60] or C substituting N (C_N) - related defects [60–62]. This type of YL emission is absent in the GaN NCs, indicating that a higher crystalline quality of GaN is obtained in the NC structure.

Finally, the HVPE-GaN reference sample and sample FS006 were subject to 77 K μ-PL measurements, and the results are shown in Fig. 7(b). The NC sample demonstrates a strong band edge emission from the GaN wurtzite crystal observed at 357 nm. In addition, the emission peak at 378 nm (3.28 eV) comes from donor-acceptor pairs (DAP) recombinations, while the weaker peak at 388 nm (3.19 eV) is 1-longitudinal optical (LO) phonon replica [64–66]. The DAP recombinations can be observed despite only Si (donor) atoms were used as dopant and probably involve acceptor levels related to carbon impurities, specifically C_N [67].

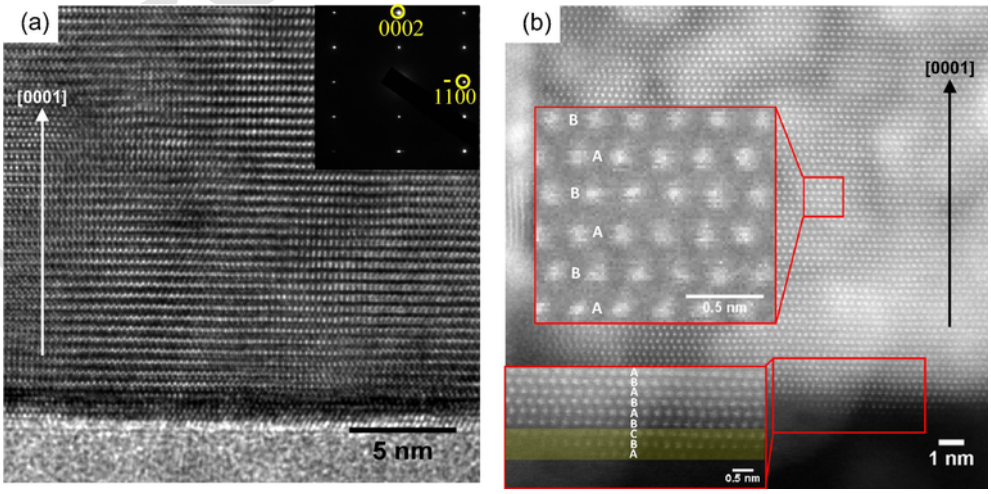

Fig. 6. (a) HRTEM and SAED (inset) of a GaN NC (from sample FS006) including its interface with the fused silica substrate, showing a thin interfacial layer (dark contrast). (b) Aberration corrected HAADF STEM image of the GaN NC (upper inset: crystal stacking order of wurtzite, lower inset: interface layer).

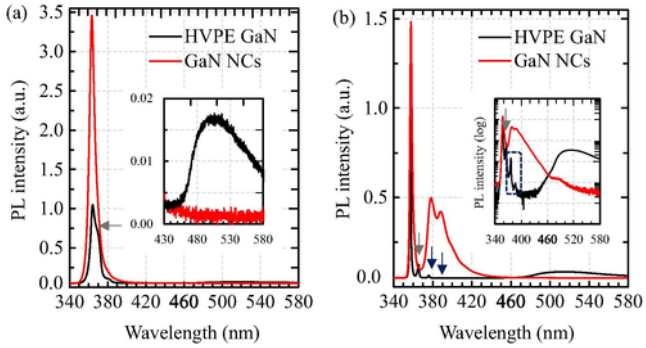

Fig. 7. PL spectra of a HVPE-GaN reference sample (black line) and an ensemble of GaN NCs (sample FS006, red line) measured at (a) RT (inset: linear scale in the range from 430 to 580 nm) and (b) 77 K (inset: logarithmic scale). In HVPE GaN: grey arrow indicates exciton bound to structural defects [63] and blue arrow (inset: blue dashed box) marks donor acceptor pair recombinations. (For interpretation of the references to colour in this figure legend, the reader is referred to the web version of this article.)

That GaN material with columnar structure is marked by a prominent intensity of DAP luminescence and their 1-LO phonon replica, as compared to the HVPE GaN reference sample (marked by blue arrows in Fig. 7(b), might be explained by the presence of unintentional C atoms in the chamber, enforcing incorporation of C into the N sublattice during growth. On the other hand, the halide vapor precursor of the HVPE technique is known to give high purity materials without carbon contamination [68]. Secondary ion mass spectroscopy (SIMS) measurement reveals that in the case of another GaN NC sample, C atoms are present in the n-GaN NCs part at a concentration level of ca. one order of magnitude lower than Si, i.e. 10^{16} C atoms/cm^3 and 10^{17} Si atoms/cm^3. Quantitative SIMS analysis on sample FS006 in particular can be suggested as further research topic. Nevertheless, although the concentration level of unintentional C atoms is relatively high, defects which might originate from C_{Ga} [57,60] or C_N [60–62] are effectively quenched, confirmed from the lacking of YL emission in the GaN with NC structure.

Furthermore, there is a weak PL peak at 365 nm in the HVPE-GaN reference sample (grey arrow) which transforms into a PL shoulder around 369 nm in the RT μ-PL spectrum. This peak is affiliated with an exciton bound to structural defects [63]. The absence of any zinc blende GaN band-edge and YL emission [69] are evidence of the exceptionally high crystal quality of the GaN NCs in sample FS006.

4. Conclusions

The morphology and optical quality of GaN NC structures grown on fused silica glass substrates using PA-MBE have been systematically studied as a function of substrate temperature, Ga flux and N_2 flow rate. Each growth condition gives rise to distinct effects towards the columnar structure. Under optimized conditions, a high density of vertically aligned self-assembled GaN NCs are successfully grown on fused silica without the aid from any external catalyst. TEM confirms a high-quality wurtzite crystal structure with the absence of threading dislocations, stacking faults and twinning defects. A layer with a zinc blende structure/stacking, probably Si_xN_y, and a thickness of a few atomic layers is formed at the interface to the glass. Both RT and 77 K μ-PL measurements show a sharp and intense GaN excitonic emission from an ensemble of NCs with the absence of any deep level related emissions, indicating a very high crystal quality of the free-standing GaN NCs grown on fused silica. These results could facilitate further development of an economical route towards the fabrication of efficient III-nitride NC-based LED devices.

Acknowledgements

We acknowledge T. Oto, I. Matsuyama and Y. Nakagawa for their fruitful discussions on the 77 K μ-PL data. This work was supported by the FRINATEK (Grant No. 214235) and NANO2021 (Grant No. 239206) programs of the Research Council of Norway and by Japan Society for the Promotion of Science KAKENHI (Grant No. 24000013). The Research Council of Norway is also acknowledged for the support to NTNU NanoLab through the Norwegian Micro- and Nano-Fabrication Facility, NorFab (Grant no. 197411), the NORTEM facility (Grant no. 197405), and the Norwegian PhD Network on Nanotechnology for Microsystems (FORSKERSKOLER-221860/F40).

References

[1] X. Liu, Y. Lu, W. Yu, J. Wu, J. He, D. Tang, Z. Liu, P. Somasuntharam, D. Zhu, W. Liu, P. Cao, S. Han, S. Chen, L. Seow Tan, AlGaN/GaN metal-oxide-semiconductor high-electron-mobility transistor with polarized P(VDF-TrFE) ferroelectric polymer gating, Sci. Rep. 5 (2015) 14092.
[2] S.J. Pearton, F. Ren, GaN Electronics, Adv. Mater. 12 (2000) 1571–1580.
[3] A. Müller, G. Konstantinidis, M. Dragoman, D. Neculoiu, A. Kostopoulos, M. Androulidaki, M. Kayambaki, D. Vasilache, GaN membrane metal-semiconductor-metal ultraviolet photodetector, Appl. Opt. 47 (2008) 1453–1456.
[4] S. Nakamura, M. Senoh, S.-I. Nagahama, N. Iwasa, T. Yamada, T. Matsushita, H. Kiyoku, Y. Sugimoto, T. Kozaki, H. Umemoto, M. Sano, K. Chocho, Continuous-wave operation of InGaN/GaN/AlGaN-based laser diodes grown on GaN substrates, Appl. Phys. Lett. 72 (1998) 2014–2016.
[5] S. Nakamura, T. Mukai, M. Senoh, Candela-class high-brightness InGaN/AlGaN double-heterostructure blue-light-emitting diodes, Appl. Phys. Lett. 64 (1994) 1687–1689.
[6] L. Liu, J.H. Edgar, Substrates for gallium nitride epitaxy, Mat. Sci. Eng.: R: Rep. 37 (2002) 61–127.
[7] F. Glas, Critical dimensions for the plastic relaxation of strained axial heterostructures in free-standing nanowires, Phys. Rev. B 74 (2006).
[8] K. Kishino, A. Kikuchi, H. Sekiguchi, S. Ishizawa, InGaN/GaN nanocolumn LEDs emitting from blue to red, Proc. SPIE 6473, Gallium Nitride Materials and Devices II, SPIE, San Jose, California, United States, 2007, pp. 64730T–64731.
[9] D.L. Dheeraj, G. Patriarche, H. Zhou, T.B. Hoang, A.F. Moses, S. Grønsberg, A.T.J. van Helvoort, B.-O. Fimland, H. Weman, Growth and characterization of wurtzite GaAs nanowires with defect-free zinc blende GaAsSb inserts, Nano Lett. 8 (2008) 4459–4463.
[10] D.L. Dheeraj, G. Patriarche, H. Zhou, J.C. Harmand, H. Weman, B.O. Fimland, Growth and structural characterization of GaAs/GaAsSb axial heterostructured nanowires, J. Cryst. Growth 311 (2009) 1847–1850.
[11] A.M. Munshi, D.L. Dheeraj, J. Todorovic, A.T.J. van Helvoort, H. Weman, B.-O. Fimland, Crystal phase engineering in self-catalyzed GaAs and GaAs/GaAsSb nanowires grown on Si(111), J. Cryst. Growth 372 (2013) 163–169.
[12] K. Tomioka, J. Motohisa, S. Hara, T. Fukui, Control of InAs nanowire growth directions on Si, Nano Lett. 8 (2008) 3475–3480.
[13] V. Kumaresan, L. Largeau, F. Oehler, H. Zhang, O. Mauguin, F. Glas, N. Gogneau, M. Tchernycheva, J.C. Harmand, Self-induced growth of vertical GaN nanowires on silica, Nanotechnology 27 (2016) 135602.
[14] L. Cerutti, J. Ristić, S. Fernández-Garrido, E. Calleja, A. Trampert, K.H. Ploog, S. Lazic, J.M. Calleja, Wurtzite GaN nanocolumns grown on Si(001) by molecular beam epitaxy, Appl. Phys. Lett. 88 (2006) 213114.
[15] K. Kishino, S. Ishizawa, Selective-area growth of GaN nanocolumns on Si(111) substrates for application to nanocolumn emitters with systematic analysis of dislocation filtering effect of nanocolumns, Nanotechnology 26 (2015) 225602.
[16] R. Colby, Z. Liang, I.H. Wildeson, D.A. Ewoldt, T.D. Sands, R.E. García, E.A. Stach, Dislocation filtering in GaN nanostructures, Nano Lett. 10 (2010) 1568–1573.
[17] H. Sekiguchi, K. Kishino, A. Kikuchi, Formation of InGaN quantum dots in regularly arranged GaN nanocolumns grown by rf-plasma-assisted molecular-beam epitaxy, Phys. Status Solidi C 7 (2010) 2374–2377.
[18] S.D. Hersee, A.K. Rishinaramangalam, M.N. Fairchild, L. Zhang, P. Varangis, Threading defect elimination in GaN nanowires, J. Mater. Res. 26 (2011) 2293–2298.
[19] X. Zhang, V.G. Dubrovskii, N.V. Sibirev, X. Ren, Analytical study of elastic relaxation and plastic deformation in nanostructures on lattice mismatched substrates, Cryst. Growth Des. 11 (2011) 5441–5448.
[20] V. Consonni, M. Knelangen, U. Jahn, A. Trampert, L. Geelhaar, H. Riechert, Effects of nanowire coalescence on their structural and optical properties on a local scale, Appl. Phys. Lett. 95 (2009) 241910.
[21] M. Sobanska, A. Wierzbicka, K. Klosek, J. Borysiuk, G. Tchutchulashvili, S. Gieraltowska, Z.R. Zytkiewicz, Arrangement of GaN nanowires grown by plasma-assisted molecular beam epitaxy on silicon substrates with amorphous Al_2O_3 buffers, J. Cryst. Growth 401 (2014) 657–660.
[22] M. Yoshizawa, A. Kikuchi, M. Mori, N. Fujita, K. Katsumi, Growth of self-organized GaN nanostructures on Al_2O_3 (0 0 0 1) by RF-radical source molecular beam epitaxy, Jpn. J. Appl. Phys. 36 (1997) L459.
[23] M. Yoshizawa, A. Kikuchi, N. Fujita, K. Kushi, H. Sasamoto, K. Kishino, Self-organization of GaN/Al0.18Ga 0.82N multi-layer nano-columns on (0 0 0 1) Al_2O_3 by RF molecular beam epitaxy for fabricating GaN quantum disks, J. Cryst. Growth 189 (1998) 138–141.
[24] T. Stoica, E. Sutter, R.J. Meijers, R.K. Debnath, R. Calarco, H. Lüth, D. Grützmacher, Interface and wetting layer effect on the catalyst-free nucleation and growth of GaN nanowires, Small 4 (2008) 751–754.
[25] S. Zhao, M.G. Kibria, Q. Wang, H.P.T. Nguyen, Z. Mi, Growth of large-scale vertically aligned GaN nanowires and their heterostructures with high uniformity on SiOx by catalyst-free molecular beam epitaxy, Nanoscale 5 (2013) 5283–5287.
[26] Y. Park, S. Jahangir, Y. Park, P. Bhattacharya, J. Heo, InGaN/GaN nanowires grown on SiO_2 and light emitting diodes with low turn on voltages, Opt. Exp. 23 (2015) A650–A656.

from nucleation to the formation of dense nanowire ensembles, Nanotechnology 27 (2016) 325601.
[29] M. Wölz, C. Hauswald, T. Flissikowski, T. Gotschke, S. Fernández-Garrido, O. Brandt, H.T. Grahn, L. Geelhaar, H. Riechert, Epitaxial growth of GaN nanowires with high structural perfection on a metallic TiN film, Nano Lett. 15 (2015) 3743–3747.
[30] G. Calabrese, P. Corfdir, G. Gao, C. Pfüller, A. Trampert, O. Brandt, L. Geelhaar, S. Fernández-Garrido, Molecular beam epitaxy of single crystalline GaN nanowires on a flexible Ti foil, Appl. Phys. Lett. 108 (2016) 202101.
[31] B.J. May, A.T.M.G. Sarwar, R.C. Myers, Nanowire LEDs grown directly on flexible metal foil, Appl. Phys. Lett. 108 (2016) 141103.
[32] H. Hayashi, Y. Konno, K. Kishino, Self-organization of dislocation-free, high-density, vertically aligned GaN nanocolumns involving InGaN quantum wells on graphene/SiO_2 covered with a thin AlN buffer layer, Nanotechnology 27 (2016) 055302.
[33] M. Heilmann, A.M. Munshi, G. Sarau, M. Göbelt, C. Tessarek, V.T. Fauske, A.T.J. van Helvoort, J. Yang, M. Latzel, B. Hoffmann, G. Conibeer, H. Weman, S. Christiansen, Vertically oriented growth of GaN nanorods on Si using graphene as an atomically thin buffer layer, Nano Lett. 16 (2016) 3524–3532.
[34] Y. Zhao, X. Li, W. Wang, B. Zhou, H. Duan, T. Shi, X. Zeng, N. Li, Y. Wang, Growth and properties of GaAs nanowires on fused quartz substrate, J. Semicond. 35 (2014) 093002.
[35] K. Iwata, H. Asahi, K. Asami, R. Kuroiwa, S.-I. Gonda, Gas source molecular beam epitaxy growth of GaN on C- A-, R- and M-Plane sapphire and silica glass substrates, Jpn. J. Appl. Phys. 36 (1997) L661.
[36] K. Iwata, H. Asahi, K. Asami, A. Ishida, R. Kuroiwa, H. Tampo, S. Gonda, S. Chichibu, Promising characteristics of GaN layers grown on amorphous silica substrates by gas-source MBE, J. Cryst. Growth 189–190 (1998) 218–222.
[37] H. Asahi, K. Iwata, H. Tampo, R. Kuroiwa, M. Hiroki, K. Asami, S. Nakamura, S. Gonda, Very strong photoluminescence emission from GaN grown on amorphous silica substrate by gas source MBE, J. Cryst. Growth 201–202 (1999) 371–375.
[38] K. Iwata, H. Asahi, K. Asami, R. Kuroiwa, S. Gonda, Strong photoluminescence emission from GaN grown on amorphous silica substrates by gas source MBE, J. Cryst. Growth 188 (1998) 98–102.
[39] Y. Sato, A. Fujiwara, S. Ishizaki, S. Nakane, Y. Murakami, Morphologies and photoluminescence properties of GaN-based thin films grown on non-single-crystalline substrates, Phys. Status Solidi C 14 (2017) 1600151.
[40] S.-Y. Bae, J.-W. Min, H.-Y. Hwang, K. Lekhal, H.-J. Lee, Y.-D. Jho, D.-S. Lee, Y.-T. Lee, N. Ikarashi, Y. Honda, H. Amano, III-nitride core–shell nanorod array on quartz substrates, Sci. Rep. 7 (2017) 45345.
[41] J.H. Choi, J. Kim, H. Yoo, J. Liu, S. Kim, C.-W. Baik, C.-R. Cho, J.G. Kang, M. Kim, P.V. Braun, S. Hwang, T.-S. Jung, Heteroepitaxial growth of GaN on unconventional templates and layer-transfer techniques for large-area flexible/stretchable light-emitting diodes, Adv. Opt. Mater. 4 (2016) 505–521.
[42] D.P. Bour, N.M. Nickel, C.G. Van de Walle, M.S. Kneissl, B.S. Krusor, P. Mei, N.M. Johnson, Polycrystalline nitride semiconductor light-emitting diodes fabricated on quartz substrates, Appl. Phys. Lett. 76 (2000) 2182–2184.
[43] H. Peter, M. Atsuyoshi, K. Norikatsu, H. Kazumasa, S. Nobuhiko, Characterization of the shallow and deep levels in Si doped GaN grown by metal-organic vapor phase epitaxy, Jpn. J. Appl. Phys. 33 (1994) 6443.
[44] S. Ruvimov, Z. Liliental-Weber, T. Suski, J.W.A. III, J. Washburn, J. Krueger, C. Kisielowski, E.R. Weber, H. Amano, I. Akasaki, Effect of Si doping on the dislocation structure of GaN grown on the A-face of sapphire, Appl. Phys. Lett. 69 (1996) 990–992.
[45] N. Shuji, M. Takashi, S. Masayuki, Si- and Ge-doped GaN films grown with GaN buffer layers, Jpn. J. Appl. Phys. 31 (1992) 2883.
[46] S. Fernández-Garrido, J. Grandal, E. Calleja, M.A. Sánchez-García, D. López-Romero, A growth diagram for plasma-assisted molecular beam epitaxy of GaN nanocolumns on Si(1 1 1), J. Appl. Phys. 106 (2009) 126102.
[47] J. Ristić, E. Calleja, S. Fernández-Garrido, L. Cerutti, A. Trampert, U. Jahn, K.H. Ploog, On the mechanisms of spontaneous growth of III-nitride nanocolumns by plasma-assisted molecular beam epitaxy, J. Cryst. Growth 310 (2008) 4035–4045.
[48] T. Tabata, J. Paek, Y. Honda, M. Yamaguchi, H. Amano, Stacking faults and luminescence property of InGaN nanowires, Jpn. J. Appl. Phys. 52 (2013) 08JE06.
[49] K. Yamada, H. Asahi, H. Tampo, Y. Imanishi, K. Ohnishi, K. Asami, Strong photoluminescence emission from polycrystalline GaN layers grown on W, Mo, Ta, and Nb metal substrates, Appl. Phys. Lett. 78 (2001) 2849–2851.
[50] F. Furtmayr, M. Vielemeyer, M. Stutzmann, J. Arbiol, S. Estradé, F. Peirò, J.R. Morante, M. Eickhoff, Nucleation and growth of GaN nanorods on Si (1 1 1) surfaces by plasma-assisted molecular beam epitaxy - the influence of Si- and Mg-doping, J. Appl. Phys. 104 (2008) 034309.
[51] A. Wierzbicka, Z.R. Zytkiewicz, S. Kret, J. Borysiuk, P. Dluzewski, M. Sobanska, K. Klosek, A. Reszka, G. Tchutchulashvili, A. Cabaj, E. Lusakowska, Influence of substrate nitridation temperature on epitaxial alignment of GaN nanowires to Si(1 1 1) substrate, Nanotechnology 24 (2013) 035703.
[52] E. Calleja, M.A. Sánchez-García, F.J. Sánchez, F. Calle, F.B. Naranjo, E. Muñoz, S.I. Molina, A.M. Sánchez, F.J. Pacheco, R. García, Growth of III-nitrides on Si(1 1 1) by molecular beam epitaxy doping, optical, and electrical properties, J. Cryst. Growth 201 (1999) 296–317.
[53] K. Hestroffer, C. Leclere, V. Cantelli, C. Bougerol, H. Renevier, B. Daudin, In situ study of self-assembled GaN nanowires nucleation on Si(1 1 1) by plasma-assisted molecular beam epitaxy, Appl. Phys. Lett. 100 (2012) 212107.
[54] C. Chèze, L. Geelhaar, A. Trampert, H. Riechert, In situ investigation of self-induced GaN nanowire nucleation on Si, Appl. Phys. Lett. 97 (2010) 043101.
[55] D.B. Williams, C.B. Carter, Transmission Electron Microscopy: A Textbook for Materials Science, Springer, NY, 2009.
[56] D.J. As, F. Schmilgus, C. Wang, B. Schöttker, D. Schikora, K. Lischka, The near band edge photoluminescence of cubic GaN epilayers, Appl. Phys. Lett. 70 (1997) 1311–1313.
[57] J. Neugebauer, C.G. Van de Walle, Gallium vacancies and the yellow luminescence in GaN, Appl. Phys. Lett. 69 (1996) 503–505.
[58] E. Calleja, F.J. Sánchez, D. Basak, M.A. Sánchez-García, E. Muñoz, I. Izpura, F. Calle, J.M.G. Tijero, J.L. Sánchez-Rojas, B. Beaumont, P. Lorenzini, P. Gibart, Yellow luminescence and related deep states in undoped GaN, Phys. Rev. B 55 (1997) 4689–4694.
[59] M.A. Reshchikov, H. Morkoç, Luminescence properties of defects in GaN, J. Appl. Phys. 97 (2005) 061301.
[60] M.A. Reshchikov, D.O. Demchenko, A. Usikov, H. Helava, Y. Makarov, Carbon defects as sources of the green and yellow luminescence bands in undoped GaN, Phys. Rev. B 90 (2014) 235203.
[61] J.L. Lyons, A. Janotti, C.G. Van de Walle, Carbon impurities and the yellow luminescence in GaN, Appl. Phys. Lett. 97 (2010) 152108.
[62] U. Birkle, M. Fehrer, V. Kirchner, S. Einfeldt, D. Hommel, S. Strauf, P. Michler, J. Gutowski, Studies on carbon as alternative P-type dopant for gallium nitride, MRS Proc. 537 (2011).
[63] S. Fischer, G. Steude, D.M. Hofmann, F. Kurth, F. Anders, M. Topf, B.K. Meyer, F. Bertram, M. Schmidt, J. Christen, L. Eckey, J. Holst, A. Hoffmann, B. Mensching, B. Rauschenbach, On the nature of the 3.41 eV luminescence in hexagonal GaN, J. Cryst. Growth 189–190 (1998) 556–560.
[64] R. Dingle, M. Ilegems, Donor-acceptor pair recombination in GaN, Solid State Commun. 9 (1971) 175–180.
[65] H.G. Grimmeiss, B. Monemar, Low-temperature luminescence of GaN, J. Appl. Phys. 41 (1970) 4054–4058.
[66] B. Gil, Low-Dimensional Nitride Semiconductors, Oxford University Press, 2002.
[67] C. Tablero, Ionization energy levels in C-doped InxGa1 − xN alloys, Appl. Phys. Lett. 97 (2010) 192102.
[68] A. Koukitu, Y. Kumagai, Hydride Vapor Phase Epitaxy of GaN, in: D. Ehrentraut, E. Meissner, M. Bockowski (Eds.), Technology of Gallium Nitride Crystal Growth, Springer, Berlin Heidelberg, Berlin, Heidelberg, 2010, pp. 31–60.
[69] C.-C. Chen, C.-C. Yeh, C.-H. Chen, M.-Y. Yu, H.-L. Liu, J.-J. Wu, K.-H. Chen, L.-C. Chen, J.-Y. Peng, Y.-F. Chen, Catalytic growth and characterization of gallium nitride nanowires, J. Am. Chem. Soc. 123 (2001) 2791–2798.